

## <sup>63,65</sup>Cu NMR investigation of CuGeO<sub>3</sub> single crystals: The uniform and the dimerized spin-Peierls phase

Y. Fagot-Revurat and M. Horvatić

*Grenoble High Magnetic Field Laboratory, Max-Planck-Institut für Festkörperforschung  
and Centre National de la Recherche Scientifique, Boîte Postale 166, 38042 Grenoble Cedex 9, France*

C. Berthier and J. P. Boucher

*Grenoble High Magnetic Field Laboratory, Max-Planck-Institut für Festkörperforschung  
and Centre National de la Recherche Scientifique, Boîte Postale 166, 38042 Grenoble Cedex 9, France  
and Laboratoire de Spectrométrie Physique, Université Joseph Fourier Grenoble I, Boîte Postale 87,  
38402 St.-Martin d'Hères, France*

P. Ségransan

*Laboratoire de Spectrométrie Physique, Université Joseph Fourier Grenoble I, Boîte Postale 87,  
38402 St.-Martin d'Hères, France*

G. Dhahlenne and A. Revcolevschi

*Laboratoire de Chimie des Solides, Université Paris-Sud, 91405 Orsay, France*

(Received 28 June 1996)

We report a Cu NMR study performed under high magnetic field on single crystals of the inorganic spin-Peierls CuGeO<sub>3</sub> compound, in its uniform and dimerized phases. The temperature ( $T$ ) dependence of the magnetic hyperfine shift, i.e., the local static spin susceptibility, is found to scale the macroscopic susceptibility. This allows the determination of the hyperfine coupling tensor, which can be well accounted for by the on-site coupling associated with the localized electronic spin of a Cu<sup>++</sup> ion in an approximately axially symmetric environment. The nuclear spin-lattice relaxation rate ( $T_1^{-1}$ ) in the dimerized phase is found to be activated for temperature below  $\sim T_{SP}/2$ . The magnetic-field dependence of the activation energy is in good agreement with that of the energy gap determined by neutron inelastic scattering. In the uniform phase, neither the magnitude of  $T_1^{-1}$  (an order of magnitude smaller) nor its  $T$  dependence (approximately linear in  $T$  instead of being nearly constant) correspond to the theoretical predictions for a simple  $S=1/2$ , one-dimensional Heisenberg antiferromagnet, unless we admit for a filtering of the antiferromagnetic fluctuations, due to a small supertransferred hyperfine coupling. As expected, we found no magnetic-field dependence of  $T_1$  ( $T \geq 1.5 T_{SP}$ ) in the range 8.9–14.9 T. [S0163-1829(97)05105-9]

### I. INTRODUCTION

It is well established that the inorganic compound CuGeO<sub>3</sub> (Ref. 1) provides a good example of a spin-Peierls (SP) transition.<sup>2,3</sup> This phenomenon is characterized by different structural distortions that are expected to be induced by the quantum fluctuations of the spin system which is coupled to the lattice. Such a dynamic magnetoelastic effect has been predicted to occur essentially in the one-dimensional (1D) Heisenberg (or XY) antiferromagnetic (AF)  $S=1/2$  spin chains.<sup>4</sup> The observation of the SP transitions was obtained previously on organic materials, and they have been widely investigated in the 1980's.<sup>2,5</sup> In contrast to the case of organic compounds, the structure of CuGeO<sub>3</sub> is relatively simple, and large high-purity single crystals can be synthesized.<sup>6</sup> This has enabled experimentalists to perform and develop measurements including those which could not have been done before as, e.g., detailed studies by neutron scattering.<sup>7,8</sup> As a consequence, a large activity, both theoretical and experimental, has been devoted to this compound recently. In the present work we report a nuclear magnetic resonance (NMR) investigation on single crystals, providing

accurate insights in magnetic properties; local microscopic static ( $\chi$ ) and dynamic ( $\chi''$ ) magnetic susceptibility are measured through the magnetic hyperfine shift ( $K$ ) and the nuclear spin-lattice relaxation rate ( $T_1^{-1}$ ), directly at the position of (copper) spins.

The phase diagram of CuGeO<sub>3</sub> is shown in Fig. 1; as a function of magnetic field ( $H$ ) and temperature ( $T$ ) three different phases characterizing a SP system are well identified. At high temperature there is a "uniform" ( $U$ ) phase where the spins system is considered to be made of regular magnetic chains, defined by one lattice constant  $c$  and one exchange coupling between neighboring spin ( $J$ ). As the temperature is lowered, a structural transition is achieved at  $T_{SP}$  ( $T_{SP} \cong 14$  K at zero field); in moderate magnetic field this transition corresponds to a dimerization of the lattice,<sup>9</sup> so that the separation between nearest neighbors is now given by  $c \pm \delta_c$  and the exchange coupling by  $J \pm \delta_J$ . In this way an energy gap is opened in the otherwise gapless spectrum of the spin excitations, allowing for a magnetic energy gain which outweighs the loss in elastic energy. Starting from this dimerized ( $D$ ) phase, increasing the magnetic-field value induces another phase transition at the critical field  $H_c \cong 12.5$

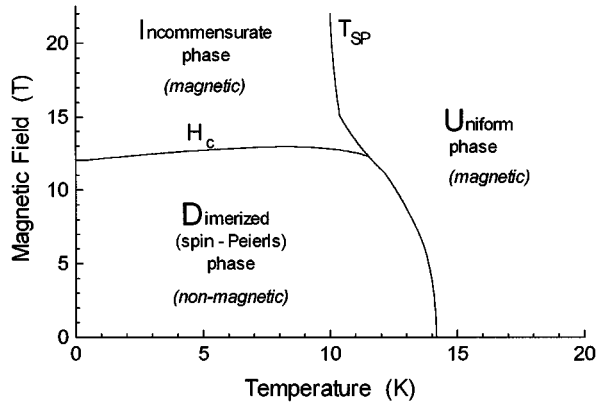


FIG. 1. The phase diagram of CuGeO<sub>3</sub>.

T. This field-induced transition corresponds to a new deformation of the lattice, which becomes incommensurate<sup>10</sup> ( $I$ ). This defines the  $I$  phase. This paper gives a rather complete account of the NMR results in the  $U$  and  $D$  phases, while data showing the solitonlike spin-density distribution in the  $I$  phase have been reported elsewhere.<sup>11</sup>

In the SP phenomenon, the magnetic field plays a crucial role, which is clearly shown by the phase diagram of Fig. 1. From the theoretical point of view, there is also a particular interest in the field dependence studies of this system; the SP Hamiltonian can be mapped by the Jordan-Wigner transformation onto a 1D system of interacting spinless fermions, and the variation of magnetic field corresponds to a change of the chemical potential, i.e., of the filling of the band. Our NMR measurements offer the possibility to probe the dynamics of the  $U$  and  $D$  phases at relatively large field values (6.6–14.9 T), and to compare these results to the published zero-field data. For analyzing the  $U$  phase, we shall refer explicitly to the standard model of Heisenberg AF spin-1/2 chain. At low temperature ( $k_B T < J$ ), such system is known to develop large quantum fluctuations at low energy ( $E \sim 0$ ). However, a distinction has to be made between two types of fluctuations: (i) those which are associated with the AF short-range order develop at the AF wave vector  $q \sim \pi/c$ , and are expected to be dominant. (ii) The uniform fluctuations, i.e., those associated with short wave vectors  $q \sim 0$ , are expected to be negligible at zero temperature and to increase with the temperature. Our analysis shows that both types of fluctuations contribute to the NMR  $T_1^{-1}$  relaxation rate in the  $U$  phase. In the  $D$  phase, a completely different situation is found, and reference has to be made to the more general concept of “spin-liquid” systems, to which the dimerized, but also the Haldane and ladder spin chain belong. In these systems, the elementary spin excitations show an energy gap (with respect to the ground state), and they are also defined by an extra quantum number  $S=1$ , where  $S$  is the total spin value. As a consequence, different relaxation processes are expected to occur, some of them being strongly field dependent.

Our measurements in CuGeO<sub>3</sub> are performed on the copper nuclear spins, probing thus directly the on-site electronic  $S=1/2$  spin sites. Unfortunately, this makes the NMR investigation difficult to perform for several reasons: there are two copper sites in the system differing by the orientation of the

local environment, the anisotropy of the hyperfine coupling is very strong ( $\sim 10$ ), and the spin-spin relaxation rate ( $T_2^{-1}$ ) is fast and anisotropic. A detailed discussion of these problems is given in Sec. II. A quantitative analysis of the  $T_1^{-1}$  relaxation rate requires also an accurate determination of the hyperfine coupling tensor. This is achieved by a careful analysis of our rather complete study of the magnetic hyperfine shift, presented in Sec. III; the results are typical for localized copper electronic spin, and may be used as a reference for other NMR studies of magnetic materials. They are essentially the same as those obtained by Itoh and collaborators from the investigation of powder spectra,<sup>12</sup> and from the low-field single-crystal study<sup>13</sup> performed in parallel to this work. The NMR, i.e., the high magnetic-field measurement of  $T_1^{-1}$  in the  $U$  and  $D$  phases are presented and analyzed in Secs. IV and V, respectively. In Sec. V, the low-temperature data in the  $D$  phase are used to reveal the magnetic-field dependence of the gap in the spin excitations. Section VI contains the concluding remarks.

## II. EXPERIMENT

An essential point when performing high-field NMR in a single crystal is the understanding of the local symmetry of the site under study, which determines the proper choice of the orientation of the magnetic field with respect to the crystalline axis of the sample. In our case, although the global symmetry of CuGeO<sub>3</sub> is orthorhombic, the local symmetry of the copper site is lower. The only element of symmetry is a mirror plane, perpendicular to the  $c$  axis (chain direction), which can thus be *a priori* identified<sup>14</sup> as one of the principal axes of the electric-field-gradient (EFG) tensor and the magnetic hyperfine shift ( $K$ ) tensor. To determine the two other principal axes, we are helped by the approximate symmetry of the local environment of the copper; each Cu<sup>++</sup> ion is surrounded by six oxygens in a *distorted* octahedral coordination. The nearest neighbors (NN) are four O(2) sites forming a rectangle (“nearly” a square) whose sides differ by 15%. The top and the bottom apex of the “octahedron” are the O(1) sites laying on the O(1)-Cu-O(1) line which is somewhat (by 6°) canted from the normal to the plane of the O(2) rectangle. Neglecting the distortions of the octahedron one would naturally think that the Cu<sup>++</sup> ion possesses an electronic hole in the  $d_{x^2-y^2}$  orbital pointing towards the O(2) sites, with the EFG and  $K$  tensors of axial symmetry with respect to the normal to the O(2) plane. Indeed, this turns out to be a good approximation. Low-field ( $\leq 1.1$  T) NMR experiments performed on a single crystal<sup>15</sup> have allowed the determination of the principal  $Z$  axis of the EFG tensor as laying in between the O(1)-Cu-O(1) line and the normal to the NN O(2) plane. The anisotropy of the tensor is relatively weak,  $\eta=0.16$ , the smallest value of the EFG tensor corresponding to the  $c$  axis ( $X$  direction). A combined interpretation of the NMR data obtained on powder,<sup>12</sup> on single crystal at low field,<sup>13</sup> and our high-field single-crystal data presented in the following section, shows that the  $K$  tensor corresponds well to the on-site hyperfine coupling to an electronic spin in a  $d_{x^2-y^2}$  orbital.

In order to define the whole  $K$  tensor we used only two characteristic orientations of the single crystal in the external magnetic field  $H_0$ , namely  $H_0 \parallel X=c$  axis and  $H_0 \parallel Z$  axis. In

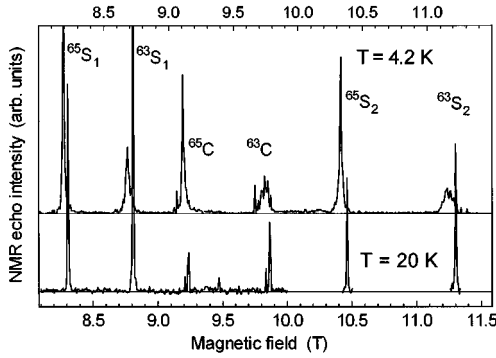


FIG. 2. Field-sweep Cu NMR spectra of the dimerized ( $T=4.2$  K,  $\nu_0=112.2$  MHz) and the uniform ( $T=20$  K,  $\nu_0=113.2$  MHz) phase, with the magnetic field  $H_0\parallel c$  axis. For each of the two isotopes  $^{63}\text{Cu}$  and  $^{65}\text{Cu}$ , the symbols  $C$ ,  $S_1$ ,  $S_2$  denote the central line and two satellites, respectively. The field-sweep scales of the two spectra are slightly shifted so that, within the resolution of the figure, we see the line positions as if they were taken at the same frequency.

the former case both Cu sites are equivalent and we recover  $6=2\times 3$  NMR lines corresponding to two copper isotopes  $^{63}\text{Cu}$  and  $^{65}\text{Cu}$  having nuclear spin  $I=3/2$ , as shown in Fig. 2. For the other orientation, it must be noticed that two adjacent copper sites along the  $b$  direction have different  $Z$  axes, which can be obtained by rotating the  $b$  axis of the crystal by  $\vartheta_0=\pm 37.5^\circ$  around  $X=c$  axis.<sup>15</sup> (This is confirmed by recent determination<sup>13</sup> yielding  $\vartheta_0=\pm 36.2^\circ$ .) Thus, when  $H_0$  is aligned along the  $Z$  axis for one site, it makes an angle  $2\vartheta_0$  with the local  $Z$  axis of the other one (in the  $Z$ - $Y$  plane). The resulting spectrum, shown in Fig. 3, contains  $2\times 6=12$  NMR lines corresponding to both orientations. The spectra shown in Figs. 2 and 3 have allowed us to confirm the determination of the EFG tensor for Refs. 15, 16, 12, 13, and to extract the complete  $K$  tensor at two temperatures that are characteristic for the  $U$  and  $D$  phase, as given in Table I. It turns out that the broad lineshape of the  $2\vartheta_0$  lines in Fig. 3 corresponds to a rather important misorientation (mosaicity) of the cleavage ( $b,c$ ) planes in our single crystal, with a distribution of angles spread over  $5^\circ$ . For all other lines the magnetic field was (nearly) parallel to one of the principal axes of the EFG tensor, making the lines insensitive to small misorientation, since for these directions the linear term in the angular dependence of the line position is zero.<sup>14</sup>

The present investigation of  $\text{CuGeO}_3$  has been carried out on two single crystals of approximately 100 mg. The measured temperature dependences of the magnetic susceptibility are typical of good quality samples, showing a spin-Peierls transition at  $T_{\text{SP}}=14$  K (at 1 T). Sample 1 was used for all the measurements with  $H_0\parallel Z$  axis and, as discussed

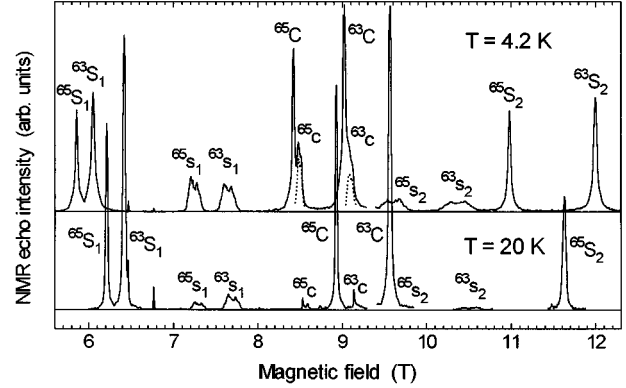


FIG. 3. Field-sweep Cu NMR spectra of the dimerized ( $T=4.2$  K) and the uniform ( $T=20$  K) phase, taken at 103.3 MHz, with the magnetic field  $H_0\perp c$  axis and at  $37.5^\circ$  to  $b$  axis. For each of the two isotopes  $^{63}\text{Cu}$  and  $^{65}\text{Cu}$ , the symbols  $C$ ,  $S_1$ ,  $S_2$  and  $c$ ,  $s_1$ ,  $s_2$  denote the central line and two satellites corresponding to two orientations  $\theta=0^\circ$  and  $\theta=75^\circ$ ,  $\phi=90^\circ$ , respectively. Dotted lines represent the reconstruction of the  $c$  lines, where  $C$  lines are taken to be symmetrical.

above, the spectrum shown in Fig. 3 reveals a rather important mosaicity. For the measurements with  $H_0\parallel X$  axis, a configuration in which the spectra are *a priori* more sensitive to the mosaicity, another sample (2) with less mosaicity has been chosen. The better quality of sample 2 has been confirmed by performing several comparative tests with  $H_0\parallel Z$  axis, not shown in this paper; the only observed difference as compared to sample 1 was significantly sharper NMR lines.

Another important ‘‘technical’’ point in this investigation is a very fast spin-spin relaxation rate  $T_2^{-1}$  which makes the NMR spin-echo resonance difficult to observe. Moreover, the strong anisotropy of the hyperfine coupling tensor is reflected in the anisotropy of the  $T_2^{-1}$ , making, e.g., the NMR resonance in the  $U$  phase hardly observable for any direction away from the  $Z$  axis. In the spectra shown in Figs. 2 and 3 one can see that the loss of signal due to the spin-spin relaxation modifies the relative intensities of the lines making it more easy to observe the satellite lines as compared to the central line, isotope  $^{65}\text{Cu}$  as compared to  $^{63}\text{Cu}$ , and spectra with  $H_0\parallel Z$  direction as compared to those corresponding to other  $H_0$  directions. All these experimental findings are in fact a direct consequence of the strong anisotropy of hyperfine coupling  $R=A_z/A_\perp\sim 9\gg 1$ . For such an anisotropic on-site hyperfine coupling tensor, and a relaxation of pure magnetic origin, one can estimate the anisotropy of  $T_1^{-1}$  to be  $T_{1\perp}^{-1}/T_{1z}^{-1}\cong R^2/2$ . The corresponding lifetime contribution to the spin-spin relaxation rate, the so-called Redfield contribution, then becomes  $T_{2R_z}^{-1}\cong (R^2/2)T_{1z}^{-1}$ , and its anisotropy

TABLE I. The copper magnetic hyperfine shift ( $K$ ) and coupling ( $A$ ) tensors determined from the spectra shown in Figs. 2 and 3.  $\Delta K=K(20\text{ K})-K(4.2\text{ K})$ . The experimental error is  $\pm 0.05\%$  or  $\pm 4$  kOe.

Axis	$K(4.2\text{ K})$ (%)	$K(20\text{ K})$ (%)	$\Delta K$ (%)	$\Delta\chi$ ( $10^{-3}$ emu/mol)	$A$ (kOe)
$Z$	1.54	-4.25	-5.79	1.63	-478
$Y$	0.26	-0.35	-0.61	1.13	-60
$X=c$	0.31	-0.17	-0.48	1.21	-46

$T_{2R_{\perp}}^{-1}/T_{2R_Z}^{-1} \cong 3.5$  and  $2.5$  for the central and the satellite lines, respectively. The dominant, spin-spin contribution to  $T_2^{-1}$  ( $T_{2G}^{-1}$ ) is proportional to  $\gamma^2 \sqrt{n}$ , where  $\gamma$  is the gyromagnetic ratio and  $n$  the natural abundance of the Cu isotope, a product which is 1.30 times smaller for the  $^{65}\text{Cu}$  isotope than for the  $^{63}\text{Cu}$  one. The anisotropy of the spin-spin contribution  $T_{2G_{\perp}}^{-1}/T_{2G_Z}^{-1}$  is expected to be  $\leq 2$  and  $1.5$  for the central and the satellite lines, respectively, where the given numbers are upper values corresponding to the case where *all* the spins can be considered as ‘‘like’’, i.e., participating in the  $I_+I_-$  exchange process.<sup>17</sup>

In the  $T=4.2$  K spectrum shown in Fig. 2 one can also see an unexpected difference between the two copper isotopes: the NMR lines corresponding to the more abundant  $^{63}\text{Cu}$  isotope (69.1%) are much wider than those corresponding to  $^{65}\text{Cu}$ , and their line shape presents distinct oscillations which are not an experimental artifact. We think that this is related to the very strong indirect spin-spin interaction and should be considered as an interesting technical point, which is out of the scope of our study. Most of the results presented here have been obtained on  $^{65}\text{Cu}$  isotope, where this effect is not visible, probably due to the smaller natural abundance (30.9%).

Note that in performing NMR studies in single crystals, the large value of  $T_2^{-1}$  brings an important loss of signal intensity, while its anisotropy distorts the relative intensity of the NMR lines, but this does not affect the shape or the position of the lines, which are important for the determination of the  $K$  tensor and the local magnetic-field distribution. However, in the interpretation of powder spectra these deformations are likely to be more inconvenient. Moreover, the linewidth of the lines increases more than one order of magnitude near  $T_{\text{SP}}$ ,<sup>18</sup> which is again less harmful for the determination of the center of the line in the study of single crystals, in comparison to the shift determination from the position of the singularities in the powder spectra. We believe that minor differences in the  $K$  values found here and reported in Ref. 12 should be related to these problems.

The signal loss due to large values of  $T_2^{-1}$  is particularly important in the  $U$  phase, where we were obliged to put the echo (i.e., the signal) within the ring-down time after the  $\pi$  pulse ( $\tau \sim 5 \mu\text{s}$ ). While the corresponding modifications in the NMR spectra are not important for the interpretation, as discussed above, the effects are much more harmful for the  $T_1$  determination. In short, measurements in the  $U$  phase could be performed only for  $H_0 \parallel Z$  axis where both  $T_1$  and  $T_2$  are significantly longer than for other orientations of the field. Although our attempt to determine  $T_{1x}$  was unsuccessful, it proved that reliable  $T_1$  measurements with  $H_0 \perp Z$  axis are not hopeless, but require special efforts in order to reduce the pulse lengths, ring-down time (e.g., using active damping), and the dead time of the receiver, significantly below standard values.

Spin-lattice relaxation rate measurements have been performed in the configuration  $H_0 \parallel Z$  axis, on the central line, i.e.,  $(1/2, -1/2)$  transition of  $^{65}\text{Cu}$ , as this isotope corresponds to a longer  $T_2$  value and to a better separation between the NMR lines corresponding to two sites (Fig. 3). Only the 14.9 T data were taken on  $^{63}\text{Cu}$  isotope, and scaled to  $^{65}\text{Cu}$  data by applying the correction factor

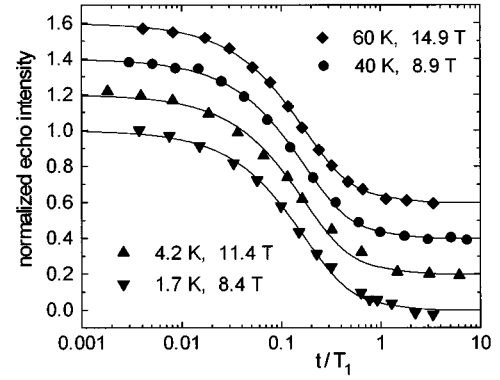


FIG. 4. Normalized time dependence of the longitudinal magnetization in the  $T_1$  measurements. Representative data shown in the figure cover full span of  $T_1$ 's, ranging from 1.1 ms at 60 K to 80 s at 1.7 K, and several values of magnetic field. The full lines are the standard fit to  $S(t) \propto 0.9e^{-6t/T_1} + 0.1e^{-t/T_1}$ , used in the determination of  $T_1$ .

$(^{65}\gamma/^{63}\gamma)^2 = 1.147$ . (It has been shown<sup>16</sup> that the relaxation is of magnetic origin). The same conversion has been used to convert the published NQR data.<sup>16,12</sup>  $T_1$  measurements at high temperature were performed using a very reliable ‘‘differential’’ echo sequence<sup>19</sup> corresponding to the recovery after a spin-inversion pulse. For long  $T_1$ 's at low temperature, in a more standard way, we measured the recovery after a saturation comb. Both methods lead to the same time dependence of longitudinal magnetization  $S(t) \propto 0.9e^{-6t/T_1} + 0.1e^{-t/T_1}$ , as shown in Fig. 4.

### III. MAGNETIC HYPERFINE SHIFT

Figure 5 shows the temperature dependence of the position of the center of  $^{65}\text{Cu}$  ( $1/2, -1/2$ ) NMR line for  $H_0 \parallel Z$  axis, converted into the corresponding  $K_{ZZ}$  values. As the hyperfine coupling is the strongest in this direction, these data are those for which the error in the determination of the  $T$  dependence of  $K$  is minimal. These data, taken at 103.282 MHz, i.e., for magnetic field ranging from 8.4 to 8.9 T, are

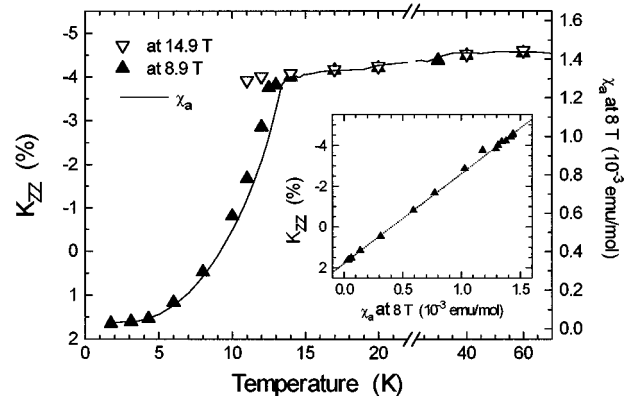


FIG. 5. Magnetic hyperfine shift  $K$  taken at 8.4–8.9 T and 14.9 T as a function of temperature, compared to the macroscopic magnetic susceptibility  $\chi_a$  data (Ref. 20) taken at 8 T. Plot of the  $K(T/12.5 \text{ K})$  vs  $\chi_a(T/13.1 \text{ K})$ , shown in the inset, reveals that linear relation holds at all values, once we take into account the difference in the transition temperatures.

compared to the macroscopic magnetization data<sup>20</sup> measured at  $H_0=8$  T|| $a$  axis and converted to magnetic susceptibility. One can notice that, apart from the small difference in the transition temperature, there is a precise linear dependence between the two quantities as revealed by the  $K_{ZZ}(T/12.5$  K) vs  $\chi_a(T/13.1$  K) plot shown in the inset of Fig. 5. Neglecting the chemical shift, we have

$$K_{\alpha\alpha}(T) = K_{\alpha\alpha}^{\text{orb}} + A_{\alpha}\chi_{\alpha}(T)/(g_{\alpha}\mu_B N_A), \quad \alpha = X, Y, Z, \quad (1)$$

where  $A_{\alpha}$  is the hyperfine coupling tensor,  $K_{\alpha\alpha}^{\text{orb}}$  is the temperature-independent orbital part of the shift, and  $N_A$  is Avogadro's constant. Thus, the NMR data show that macroscopic magnetic susceptibility corresponds to the microscopic spin susceptibility of copper electronic spins, in both  $U$  and  $D$  phases. In particular, in the  $D$  phase this confirms the dimerization in which neighboring spins couple into true singlets, with *no* local AF variation of microscopic field; in Fig. 3 we see that (away from the transition<sup>18</sup>) the width of the NMR lines is essentially the same in both phases.

Before starting the discussion on the hyperfine coupling tensor, let us remark that the difference in  $T_{\text{SP}}$  for the two measurements of Fig. 5 can be related to the magnetic field and orientation dependence of  $T_{\text{SP}}$ , the orientation dependence coming (at least) from the strong anisotropy of the Landé factor  $g$  (discussed below), as the theory predicts that  $\Delta T_{\text{SP}}(H) \propto -(g\mu_B H)^2$ . Note that the orientation dependence of  $T_{\text{SP}}(H)$  is another source of problems (in addition to the very strong increase of linewidths at  $T_{\text{SP}}$ ) in the interpretation of powder spectra, which is a possible reason why Itoh, Hirashima, and Motoya<sup>12</sup> reported some deviations from the linear dependence of Eq. (1), just below  $T_{\text{SP}}$ .

The hyperfine coupling tensor  $A_{\alpha}$  has been determined from the change of the shift values between 20 and 4.2 K, reported in Table I, compared to the corresponding variation of macroscopic susceptibility. The full  $\Delta\chi_{\alpha}$  tensor has been calculated from  $\Delta\chi_{\alpha}(8$  T) =  $1.32 \times 10^{-3}$  emu/mol,<sup>20</sup> taking into account that susceptibility data confirm that  $\chi_{\alpha}/g_{\alpha}^2$ , i.e., the spin polarization, is isotropic. The declared experimental error of  $\pm 4$  kOe on the  $A_{\alpha}$  tensor corresponds to the uncertainty on the shift values only; the real error is most probably dominated by the susceptibility data.

In order to proceed with the interpretation of the  $A_{\alpha}$  tensor, we start with the transformation of the  $g$  tensor,  $g_a=2.162$ ,  $g_b=2.266$ ,  $g_c=2.070$ ,<sup>21</sup> to the XYZ coordinate system<sup>15</sup> ( $X=c$  axis). After solving the following equations,

$$\begin{aligned} g(\phi)^2 &= g_Z^2 \cos^2 \phi + g_Y^2 \sin^2 \phi \\ g_b &= g(37.5^\circ), \quad g_a = g(52.5^\circ), \end{aligned} \quad (2)$$

one obtains<sup>15</sup> a nearly axial tensor,  $g_Z=2.407$ ,  $g_Y=2.004$ , and  $g_X=g_c=2.070$ . Taking into account the local environment of copper spin and the values of  $g$  and  $A$  tensors, it is evident that in the first approximation we can use the standard description<sup>22</sup> of a  $\text{Cu}^{++}$  ion in the crystal field of tetragonal symmetry, in which we take for the perpendicular direction the average of values for  $Y$  and  $X$  direction,  $g_{\perp}=2.037$ ,  $A_{\perp}=53$  kOe. We start with the determination of the ratio of the energy levels  $\Delta_1 = E_{yz,zx} - E_{x^2-y^2}$  and  $\Delta_0 = E_{xy} - E_{x^2-y^2}$ ,

$$\frac{\Delta_1}{\Delta_0} = \frac{g_Z - 2}{8(g_{\perp} - 2)} = K_{ZZ}^{\text{orb}}/4K_{\perp}^{\text{orb}}, \quad (3)$$

a parameter which can be determined either from the anisotropy of the  $g$  tensor,  $\Delta_1/\Delta_0=1.4$ , or from the orbital shift,  $1.7\%/ (4 \times 0.30\%) = 1.4$ . Note that the following formulas are only weakly dependent on this parameter. The standard expressions<sup>22</sup> for  $A_Z$  and  $A_{\perp}$  can be solved to obtain explicit formulas for the unknown parameters measuring the size of the  $\text{Cu}^{++}$  ion and the core-polarization contribution to the hyperfine coupling

$$A_0 = 2\mu_B \langle r^{-3} \rangle = (A_{\perp} - A_Z) \left[ \frac{6}{7} - (g_Z - 2) \left( 1 - \frac{5/56}{\Delta_1/\Delta_0} \right) \right]^{-1}, \quad (4)$$

$$A_{\text{CP}} = -A_0 \left[ \frac{-A_Z}{A_0} - \frac{4}{7} + (g_Z - 2) \left( 1 + \frac{6/56}{\Delta_1/\Delta_0} \right) \right]. \quad (5)$$

Taking  $\Delta_1/\Delta_0=1.4$ , we obtain  $A_0=891$  kOe, i.e.,  $\langle r^{-3} \rangle = 7.1 \times a_0^{-3}$ , a value which is somewhat closer to the free-ion value ( $7.5 \times a_0^{-3}$ ) than for other copper salts.<sup>22</sup> The core polarization,  $A_{\text{CP}} = -359$  kOe ( $\kappa = -A_{\text{CP}}/A_0 = 0.40$ ), is also found to be stronger than the typical value for all the transition-metal ions, i.e.,  $-250$  kOe. Taking the latter value as rather well established, we can expect that at least some part of the difference between two values is due to an isotropic supertransferred hyperfine coupling ( $B$ ) to the electronic spins on the two NN coppers, for which we can estimate an upper limit  $|-2B| \leq 100$  kOe. In fact, from the analysis of the  $T_1$  data in the  $U$  phase, given in the following section, a considerably smaller value is deduced,  $B = -11$  kOe.

To compare the  $B$  value to other available data, we first note that in the similar  $\text{CuO}_2$ -based systems there should be a relation between the spin-spin coupling  $J$  and the  $B$  hyperfine coupling, as both quantities are related to the transfer integral  $t$ . In the copper oxide high- $T_c$  superconductors the  $B$  values range from 80 kOe in  $\text{YBa}_2\text{Cu}_3\text{O}_{6+x}$  to 140 kOe in  $\text{HgBa}_2\text{Ca}_2\text{Cu}_3\text{O}_{8+\delta}$ ,<sup>23</sup> for  $J$  values which are one order of magnitude greater than in  $\text{CuGeO}_3$ . Neglecting all the differences between two systems, a first guess for the order of magnitude of  $B$  in  $\text{CuGeO}_3$  is then given by a direct scaling yielding  $|B| \sim 10$  kOe, quite in agreement with the values given above.

Note that the full  $q$ -dependent hyperfine coupling is given by

$$A_{\alpha}(q_c) = A_{\alpha} - 2B[1 - \cos(q_c c)], \quad (6)$$

and it is clear that as far as the strongest,  $Z$ -direction coupling is concerned, the  $B$  term brings a minor  $q$  dependence, reducing the coupling at the AF point  $q_c = \pi/c$  by only 9% for  $B = -11$  kOe. Note that  $A_Z(q_c)$  will provide the dominant contribution in the  $T_2$  (taken for any direction) and in the  $T_1$  for all directions away from  $Z$ . Unfortunately, the  $T_{1Z}$  values measured by NQR (Refs. 12 and 16) or NMR (this paper) are sensitive only to  $X$  and  $Y$  components of hyperfine coupling, for which the existence of such a  $B$  term leads to strong attenuation of the coupling at  $q_c = \pi/c$ , resulting in the suppression of the AF fluctuations contribution to  $T_{1Z}^{-1}$ .

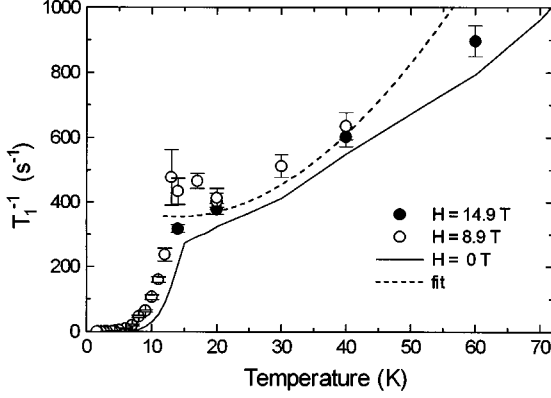


FIG. 6. Nuclear-spin-lattice relaxation rate ( $T_1^{-1}$ ) of  $^{65}\text{Cu}$  for  $H_0\parallel Z$  axis at 14.9 T and 8.9 T, and the zero-field NQR data ( $T_1^{-1} = T_{\text{INQR}}^{-1}/3$ ) of Refs. 16 and 12. The dashed line is the best fit to the numerical prediction of Sandvik (Ref. 27), where the only fit parameter is the transferred hyperfine coupling  $B = -11$  kOe.

Finally, from the orbital shift, one can deduce  $\Delta_0$  and the spin-orbit coupling parameter  $\lambda$ :

$$\Delta_0 = 16\mu_B^2 \langle r^{-3} \rangle / K_{ZZ}^{\text{orb}}, \quad (7)$$

$$\lambda = -\Delta_0(g_Z - 2)/8. \quad (8)$$

Taking  $K_{ZZ}^{\text{orb}} = 1.7\%$ , we find  $\Delta_0 = 2.4$  eV and  $\lambda = -0.12$  eV, the latter value being stronger than the free-ion value ( $-0.10$  eV).<sup>22</sup> We recall that this analysis corresponds to a simple ionic picture in which, moreover, the difference between the  $X$  (chain) and  $Y$  (perpendicular) direction has been neglected. Within these approximations, the description and the deduced parameters are quite reasonable.

In parallel to this work, Itoh *et al.*<sup>13</sup> have performed the low magnetic field study of  $\text{CuGeO}_3$  single crystals with the complete determination of  $K$  tensor. To determine the  $T$  dependence of  $K$ , they used the  $H_0\parallel b$  and  $c$ -axis data, while our values correspond to the  $H_0\parallel Z$  and  $c$ -axis configuration. Nearly the same values are found for the spin part of  $K$ , and slightly different values for the orbital part (which is more susceptible to experimental error). Itoh *et al.*<sup>13</sup> performed a full analysis of the data corresponding to the orthorhombic symmetry of the crystal field, confirming the approximation in which the departures from the tetragonal symmetry are essentially negligible. Note that within their notation the hyperfine coupling constants are divided by the corresponding  $g$  tensor values, leading to somewhat different parametrization of the data.

#### IV. UNIFORM PHASE

As already discussed at the end of Sec. II, the  $T_1$  measurements in the  $U$  phase could only be performed for the orientation  $H_0\parallel Z$  axis. Figure 6 presents a summary of the  $T_1^{-1}$  data taken at 8.9 and 14.9 T, compared to the known NQR data<sup>16,12</sup> scaled by the standard factor  $T_1^{-1} = T_{\text{INQR}}^{-1}/3$ .<sup>14</sup> The relatively important experimental error reported for the NMR data correspond to the previously discussed problems concerning the loss of the signal intensity due to very short  $T_2$ . Moreover, as the temperature approaches  $T_{\text{SP}}$ , the lines

broaden and we have detected that values of  $T_1$  depend on the position within the line shape, and observed increasing deviations from the expected form of the relaxation  $S(t)$ . All these effects are converted into declared experimental errors. Note that at 8.9 T, the value of  $T_{\text{SP}}$  is significantly higher than at 14.9 T (Fig. 1), which explains the differences observed near  $T_{\text{SP}}$ .

Away from the transition there is no difference between the  $T_1^{-1}$  data taken at 8.9 and 14.9 T, and the NMR values are essentially the same as those measured by the NQR, i.e., in zero field.<sup>16,12</sup> We conclude that there is no field dependence of the  $T_1$ , and discuss the results within the framework of theoretical results concerning the low-energy spin excitations of a spin-1/2 Heisenberg AF chain in the case of zero applied magnetic field. The excitations at  $T=0$  are then gapped everywhere for all the  $q$  vectors in the Brillouin zone but for  $q=0$  and  $q=\pi$ . Only the  $q=\pi$  mode, the spectral weight of which diverges with  $\omega \rightarrow 0$ , contributes to the nuclear spin-relaxation rate, while the  $q=0$  mode has a vanishing spectral weight. At finite temperature, the  $q=0$  mode provides a contribution which increases with temperature. Several calculations have been made to estimate the temperature dependence of the nuclear spin-lattice relaxation. In the hypothesis of a simple Heisenberg AF chain with no next-nearest-neighbor exchange interaction and a purely on-site,  $q$ -independent, hyperfine coupling, the relaxation rate can be expressed as

$$\frac{1}{T_1} = p_\beta \frac{\hbar \gamma_n^2 A_\perp^2}{J}, \quad (9)$$

where  $A_\perp^2 = (A_X^2 + A_Y^2)/2$  and  $p_\beta$  is a weakly temperature dependent prefactor of the order of 0.3–0.5. The estimate by Ehrenfreund *et al.*,<sup>24</sup> based on the fermion representation and the random-phase approximation, led to

$$p_0 = 0.306 \left[ 1 - 0.239 \left( \frac{k_B T}{J} \right)^2 \right]^{-1}. \quad (9a)$$

Going beyond the mean-field approximation, Schulz<sup>25</sup> has calculated the dominant, AF contribution to the dynamic susceptibility  $\chi''(r, t)$  and  $\chi''(q, \omega)$  using the bosonization of fermion operators in the continuum limit, and scaling arguments. In the Appendix we show that using these results,

$$p_{\text{AF}} \cong \frac{D}{\pi} \left[ 1 - \frac{4\alpha}{\pi} \frac{k_B T}{J} \right], \quad D = \pi \alpha C_\perp^2 \sim 1 - 1.5. \quad (9b)$$

The expressions for the susceptibility contain constants  $\alpha$  and  $C_\perp$  (of the order of 1) which cannot be evaluated within this approach. However, the overall prefactor  $D$  can be determined with an accuracy better than 30% using the zero temperature  $\chi''(q, T/\omega \rightarrow 0)$  limit and various sum rules,<sup>26</sup> and these estimates give several values ranging from 1 to  $\geq 1.45$ . The latter value is obtained from the static correlation function, and should be preferred in the present context. Finally, recent numerical Monte Carlo results of Sandvik<sup>27</sup> are in a very fine agreement with this value:

$$p_{\text{num}}(0.1 \leq k_B T/J \leq 0.3) \cong 0.52 \left[ 1 - 1.02 \frac{k_B T}{J} \right]. \quad (9c)$$

Numerical results confirm that the AF fluctuations decrease on increasing temperature, in accord with the discussion of analytical results of Schulz<sup>25</sup> given in the Appendix. Above  $k_B T/J \sim 0.3$ , the increasing  $q \sim 0$  contribution flattens out and reverses the temperature dependence of  $T_1^{-1}$  to a slowly increasing function.

Putting the numbers in Eq. (9c),  $J=10.2$  meV (118 K),<sup>7</sup>  $A_{\perp} = -53$  kOe, for the <sup>65</sup>Cu isotope we find (at  $k_B T/J=0.2$ ,  $p_{\text{num}}=0.41$ ) a value of  $T_1^{-1} \cong 4300$  s<sup>-1</sup>, which is expected to be nearly temperature independent, in clear disagreement with the data shown in Fig. 6. The experimental values are much smaller, and roughly linearly dependent with the temperature. The only possibility to reconcile the experimental  $T_1^{-1}$  with the simple Heisenberg AF chain, is to admit the existence of the supertransferred hyperfine coupling  $B$ , already suggested by the interpretation of  $K$  tensor, which introduces a  $q$  dependence of the hyperfine coupling given by Eq. (6). Indeed, the coupling constant for the AF fluctuations then becomes  $A_{\perp, \text{AF}}^2 = [(A_X - 4B)^2 + (A_Y - 4B)^2]/2$ , and reasonable  $B$  values could produce strong filtering ( $A_{\perp, \text{AF}}^2 \ll A_{\perp}^2$ ) of this dominant part of dynamic susceptibility. On the other hand,  $q \sim 0$  contribution strongly increases with temperature, providing a possible explanation for the experimentally observed  $T$  dependence. Using the numerical results of Sandvik,<sup>27</sup> the best fit to the data is obtained for  $B = -11$  kOe, and it is shown by the dashed line in Fig. 6. For a fit with only one adjustable parameter (i.e., the  $B$  coupling), one can see that the agreement is quite good.

Apparently the simplest way to check this hypothesis is to measure  $T_1$  with the field perpendicular to  $Z$  axis. In this case the relaxation is dominated by the  $Z$ -axis fluctuations, enhanced by the much stronger hyperfine coupling  $A_Z$ , for which the  $q$  dependence induced by the  $B$  term is essentially negligible. Unfortunately, in this case Eq. (9) predicts an extremely short  $T_1$ , with values below 10  $\mu$ s, and performing such measurements is not trivial; for example, the main characteristic time in  $S(t)$ ,  $T_1/6$ , is then of the same order as the length of the RF pulses (see also the discussion at the end of Sec. II).

## V. DIMERIZED PHASE

The principal characteristics of the dimerized phase, namely the opening of a gap in the magnetic excitations, is clearly seen in the strong decrease of  $T_1^{-1}$  below  $T_{\text{SP}}$  (Figs. 6 and 7). While the interpretation of the opening of the gap and the corresponding temperature dependence of  $T_1$  in the temperature range  $T_{\text{SP}}/2 < T < T_{\text{SP}}$  is invariably difficult, one usually expects that, below approximately  $T_{\text{SP}}/2$ , when the gap (inset to Fig. 7) and other properties of the system no longer vary with temperature,  $T_1^{-1}$  acquires an Arrhenius (or ‘‘activated’’) temperature dependence,  $T_1^{-1} \propto \exp(-E_A/k_B T)$ , reflecting only the relaxation by the thermal excitations across the gap. Indeed, as already found by NQR,<sup>16,12</sup> just below  $T_{\text{SP}}$  the  $T$  dependence of  $T_1^{-1}$  can be fitted by a power law  $T_1^{-1} \propto T^m$  where, from our NMR data, the exponent  $m(H_0=8.6 \text{ T}) = 4.7 \pm 0.1$  is somewhat smaller than the zero-field values<sup>16,12</sup>  $m(H_0=0) = 5.5$ . As shown in Figs. 7 and 8, below  $\sim 5$  K we do recover an activated behavior, with a magnetic-field dependent activation energy ( $E_A$ ). The field dependence of  $E_A$  is found to be the same as for the energy

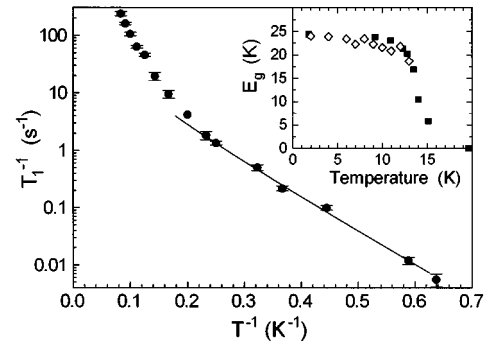


FIG. 7. The low-temperature <sup>65</sup>Cu  $T_1^{-1}$  data taken at 103.3 MHz ( $\cong 8.4$  T),  $H_0 \parallel Z$  axis, show activated behavior below 5 K, where the energy gap ( $E_g$ ) should no longer vary with temperature, as indicated by the neutron data of Refs. 7 (squares) and 8 (diamonds) shown in the inset. The full line is slightly modified exponential fit, as explained in the text.

gap ( $E_g$ ) seen by the inelastic neutron scattering,<sup>7</sup> with the magnitude of the activation energy being  $\sim 25\%$  bigger. These values are much lower than  $E_A \cong 2E_g$  predicted by Ehrenfreund and Smith<sup>28</sup> for the indirect three-magnon process. In order to explain this value of  $E_A$ , we shall consider two models, originally proposed for Haldane gap systems.

First, the phenomenological description proposed by Gaveau *et al.*<sup>29</sup> involves ‘‘one-magnon processes’’ which are usually forbidden, but allows for a finite lifetime of these excitations, due to higher-order process. The temperature dependence of  $T_1^{-1}$  is then given by  $\Gamma \exp(-E_g/T)$ , where  $\Gamma$  is the inverse of the lifetime of the ‘‘dressed magnon.’’ While, strictly speaking, Ehrenfreund and Smith<sup>28</sup> found that  $\Gamma$  varies as  $\exp(-E_g/T)$ , in Ref. 30 the  $T$  dependence of  $\Gamma$  is left as a free parameter and can be  $T$  independent (or weakly dependent) if for some reason the lifetime of the excitations is bounded by some value  $\Gamma_0$ . In this latter case one obtains the experimentally observed  $E_A = E_g$ .

The other possible mechanism was proposed by Sagi and Affleck.<sup>31</sup> They consider a relaxation mechanism, which is due to fluctuations around  $q=0$ , acting within the  $S=1$  mani-

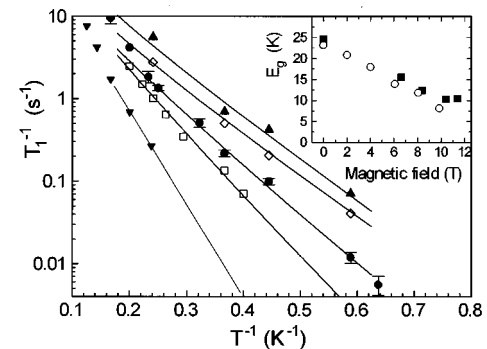


FIG. 8. The low-temperature <sup>65</sup>Cu  $T_1^{-1}$  data taken at  $H_0 \parallel Z$  axis at 6.6 T (squares), 8.4 T (circles), 10.4 T (diamonds), 11.4 T (up triangles), and 0 T NQR data of Refs. 16 and 12 (down triangles). The full lines are fits defining the corresponding energy gap, and the magnetic-field dependence of this gap is shown in the inset (solid squares), compared to the neutron data of Ref. 7 (open circles).

fold of the excitations, and can be expressed in terms of a two-magnon process. The resulting contribution to  $T_1^{-1}$  strongly depends on the symmetry of the hyperfine Hamiltonian. If the applied magnetic field is strictly parallel to the principal axis of the hyperfine coupling tensor ( $Z$  axis in our case), only transverse fluctuations of the type  $S_+(t)S_-(0)$  are effective in relaxation, which require transitions between branches of the triplet excitations, i.e.,  $\Delta m=1$  transitions. For such an interbranch process, as long as the magnon dispersion is purely parabolic and the  $q$  and field dependence of the magnon scattering matrix element is negligible on the energy scale defined by  $h=g\mu_B H$  and  $k_B T$ , the integral over the phase space for the scattering process weighted by the Boltzmann probability factor for the excitation yields:

$$1/T_{1,\text{inter}} \propto \left[ 1 + \exp\left(\frac{-h}{k_B T}\right) \right] K_0\left(\frac{h}{2k_B T}\right) \times \exp\left(-\frac{E_g(h=0) - h/2}{k_B T}\right), \quad (10)$$

where  $K_0$  is the modified Bessel function of order zero. In the high-field limit, i.e., for  $h \geq 2k_B T$ , this expression is reduced to  $1/T_{1,\text{inter}} \propto \sqrt{k_B T/h} \exp[-E_g(h=0)/k_B T]$ , presenting a field-independent activation energy, which is in clear contradiction with our experimental data. Only a low-field limit of Eq. (10) would present some field dependence of the activation energy, which is unfortunately below experimental resolution as  $h \leq E_g(h=0)$ .

However, as soon as longitudinal spin fluctuations  $S_z(t)S_z(0)$  contribute to the relaxation, intrabranched processes ( $\Delta m=0$  transitions) becomes authorized whatever is the value of the field. For each of the three branches ( $m = -1, 0, 1$ ), the contribution to the relaxation rate

$$1/T_{1,\text{intra}, m} \propto K_0\left(\frac{\hbar \omega_{\text{NMR}}}{2k_B T}\right) \exp\left(-\frac{E_{g_m}(h)}{k_B T}\right) \quad (11)$$

reflects the corresponding (field dependent for  $m = \pm 1$ ) energy gap  $E_{g_m}(h)$ , making the relaxation due to the lowest branch a good candidate for the description of our experimental data. In this formula, the nuclear spin-flip energy  $\hbar \omega_{\text{NMR}}$  provides the cutoff for the infrared divergence in the 1D integral over the phase space for the scattering process. In fact, the weak interchain coupling  $J'$  is expected to provide a more efficient cutoff of the order of  $\sqrt{JJ'}$ ,<sup>31</sup> which is unfortunately another unknown parameter modifying the  $T$  dependence of relaxation. Note that in this case, the limit  $K_0(x \ll 1) \cong \ln(2/x) - 0.5772$ , which is usually applied to Eq. (11) (Ref. 31) may no longer be valid.

In practice, one possibility to observe intrabranched fluctuations comes from a nonalignment of the magnetic field  $H_0$  with a principal axis of the hyperfine coupling tensor. In this case and for an *anisotropic* coupling, the off-diagonal elements of the coupling tensor  $A_{zx}$  and  $A_{zy}$  will be nonzero, allowing for a  $S_z(t)S_z(0)$  process. It can be shown that a misorientation of the order of a degree between  $H_0$  and the  $Z$  axis of the hyperfine coupling tensor is enough to render the intrabranched contribution larger than the interbranch one, because of the very strong anisotropy of coupling [ $(A_{zz}/A_{xx,yy})^2 \sim 100$ ] and according to the relative magnitude

of these two processes, given by the  $K_0$  functions in Eqs. (10) and (11). Since we cannot guarantee such a precision in our crystal orientation, the interbranch mechanism may very well apply to our data. By the way, Eq. (11) fits well our data up to  $H_0 \cong 10$  T.

Let us now examine in more detail the dressed one-magnon picture.<sup>29,30</sup> The relaxation rate is considered to be proportional to the (Bose) occupation number  $n(E)$  of magnetic excitations, and to the corresponding dynamic structure factor  $S(\mathbf{q}, \omega)$ :

$$T_1^{-1} \propto A_{\perp}^2 \sum_{\mathbf{q}} S(\mathbf{q}, \omega_{\text{NMR}} \sim 0) n(E_g(\mathbf{q})). \quad (12)$$

For the  $S(\mathbf{q}, 0)$  and  $E_g(\mathbf{q})$  we put the best estimates available from the neutron data. The experimental data on the  $\mathbf{q}$  dependence of the energy gap<sup>7,32</sup> are extrapolated to the complete 2D Brillouin zone by the following numerical formula given in Kelvin:

$$E_g(\mathbf{q}) = \{ \Delta^2 + (182^2 - \Delta^2) [\sin(q_c c)]^{3/2} + (67^2 - \Delta^2) [1 + \cos(q_b b)]^2 / 4 \}^{1/2}, \quad (13)$$

where the only parameter is the ‘‘gap’’ value  $\Delta = E_g(\mathbf{Q}_{\text{AF}})$  at the AF wave vector  $\mathbf{Q}_{\text{AF}} = (\pi/c, \pi/b)$ . The structure factor is approximated<sup>30</sup> by

$$S(\mathbf{q}, 0) \propto \{ [1 + (\pi - q_c \xi_c)^2] [1 + (\pi - q_b \xi_b)^2] \}^{-1/2} \times \{ \Gamma [1 + (E_g(\mathbf{q})/\Gamma)^2] \}^{-1}, \quad (14)$$

where the correlation lengths are taken to be  $\xi_c \cong 3c$  and  $\xi_b \cong b$ , as determined by neutrons.<sup>7</sup> The  $\mathbf{q}$ -dependent part of  $S(\mathbf{q}, 0)$  is taken to be<sup>7</sup> the square root of Lorentzian, corresponding to the Fourier transform (at  $\mathbf{q} \sim \mathbf{Q}_{\text{AF}}$ ) of the equal-time correlation function for an AF alternating chain:<sup>33</sup>  $\langle S_0 S_r \rangle \propto (-1)^r (r/\xi)^{-1/2} \exp(-r/\xi)$ . The energy-dependent part is described by a Lorentzian. For small damping  $\Gamma$ , ( $\Gamma \ll \Delta$ ), the Lorentzian is reduced to  $\Gamma/E_g(\mathbf{q})^2$ , and the relaxation rate is simply given by  $T_1^{-1} \propto \Gamma(T) f(\Delta, T)$ , where function  $f$  contains the sum over  $\mathbf{q}$ , which has to be evaluated numerically. Experimentally, only a weak, nonexponential  $T$  dependence of  $\Gamma(T)$  is compatible with our  $T_1^{-1}$  data, as if, e.g.,  $\Gamma$  were limited by some intrinsic value. For simplicity, in our fit we take the  $T$  independent  $\Gamma$ , which means that the temperature dependence of  $T_1^{-1}$  is described by a single fit parameter, namely the gap  $\Delta$ . These fits to the data, taken at several values of magnetic field, are shown in Figs. 7 and 8. In the inset of Fig. 8 we see that the gap values obtained in this way compare very well with neutron results, both in the magnitude and in the magnetic-field dependence.

Note that the gap values  $\Delta$  are found to be  $\sim 15\%$  lower than the activation energies  $E_A$  obtained directly from a simple Arrhenius plot. Indeed, the temperature dependence of the sum over  $\mathbf{q}$  in Eq. (12) is dominantly determined by the Boltzmann factor  $\exp(-E_g(\mathbf{q})/k_B T)$  in the occupation number  $n(E)$ . The  $E_A$  can thus be regarded as a sort of an average over  $E_g(\mathbf{q})$  taken for  $\mathbf{q} \sim \mathbf{Q}_{\text{AF}}$ , and weighted by the Boltzmann factor. Thus, Eq. (12) puts  $\Delta$  somewhat below the ‘‘raw’’  $E_A$  values. Furthermore, in the sum the dominant  $\mathbf{q}$  dependence is given by the Boltzmann factor, making the fit relatively insensitive to the model chosen for  $S(\mathbf{q}, 0)$ . In fact, if  $S(\mathbf{q}, 0)$  is replaced by a constant, the value of  $\Delta$  in the fits is decreased by only  $\sim 6\%$ .

For magnetic fields close to the transition to the  $I$  phase, our description of the relaxation rate may cease to be valid since the gap becomes comparable to the temperature and we can expect an increased contribution of the multiple magnon process.<sup>28</sup> Indeed, near  $H_c$  we find the saturation of the  $\Delta(H)$  dependence, which may be an artifact of the admixed higher processes, increasing the effective  $\Delta$  value of our fit.

In Fig. 8 we have also presented a fit showing the *tentative* extrapolation of the available NQR data<sup>16,12</sup> to lower temperature. The corresponding value of  $\Delta(H=0)$  is only an *indication* that even at zero field the gap determined by neutrons and by NQR may be the same. We remark that in zero-field the three magnon branches are superposed, which in the one- (dressed) magnon picture means that both  $m = -1$  and  $1$  branches will be active. As regards the description of two-magnon processes,<sup>31</sup> intrabranched transitions will be described by the same Eq. (11) [with  $E_g(h=0)$ , and  $\omega_{\text{NMR}}$  replaced by  $\omega_{\text{NQR}}$ ] as the intrabranched transitions, making the two processes indistinguishable. As already discussed, the frequency in the  $K_0$  function in Eq. (11) should only be regarded as the infrared-divergence cutoff frequency, which is at least  $\omega_{\text{NQR}}$  and probably much higher in reality. Furthermore, the interbranch process will be allowed only if the  $A_{\text{ZX}}$  coupling is nonzero, which will happen if the principal  $Z$  axis of the EFG gradient does not coincide with the principal axis of hyperfine coupling tensor. Altogether, it is very difficult to predict the (relative) magnitude of two possible two-magnon processes.

In conclusion, present experimental data do not allow for the conclusion about the nature of the relaxation process. Further experimental information can certainly be provided by the full angle dependence of the relaxation rate, and by extending the observed field dependence of relaxation to low magnetic field.

## VI. CONCLUSION

The single-crystal NMR data on  $\text{CuGeO}_3$  presented in this paper provide a rather complete microscopic picture of the uniform and dimerized phase, confirming and completing the results obtained on powder samples.<sup>16,12</sup> As regards the static properties, the magnetic hyperfine shift tensor and the corresponding hyperfine coupling tensor (Table I and Refs. 12 and 13) are typical for a  $\text{Cu}^{++}$  ion in a site possessing (approximate) tetragonal symmetry, with  $d_{x^2-y^2}$  orbital pointing towards the nearest-neighboring  $\text{O}(2)$  sites. However, the value of the core polarization coupling obtained from a quantitative analysis is found to be unusually high, possibly due to the presence of a small supertransferred hyperfine  $B$  term associated with the nearest neighbors. Such a term would introduce a  $q$  dependence of the hyperfine coupling, which is small for the direction of the local symmetry  $Z$  axis (perpendicular to  $d_{x^2-y^2}$  orbital), but may be very important for the perpendicular directions where the on-site coupling is of the same order. This may lead to the filtering of the AF fluctuations contribution to  $T_{1z}^{-1}$ , while the quantities for which the dominant  $Z$ -axis coupling is effective, namely  $T_{1x}$ ,  $T_{1y}$  and  $T_2$  for any direction, will be essentially unaffected by the presence of  $B$  term. Unfortunately, for technical reasons, only  $T_{1z}$  data are available so far, and we were not able to use the anisotropy of  $T_1$  as a direct way to check the hyper-

fine couplings determined from the shift data. However, when compared to the simple Heisenberg chain, the unexpectedly low  $T_{1z}^{-1}$  values and its quasilinear  $T$  dependence are suggestive of a filtering of the AF fluctuations. The observed temperature dependence should then be associated with the  $q=0$  contribution, which has been shown<sup>27</sup> to increase with temperature. In addition to that, we may also expect a modification of  $T_1$  due to various reasons: coupling to the phonons, interchain coupling, or next-nearest neighboring spin coupling (if it is important). Note that the interchain coupling is found to be as large as  $J/10$  in the  $b$  direction (and  $J/100$  in the  $a$  direction).<sup>7</sup> The possibility that the spin-Peierls transition in  $\text{CuGeO}_3$  is not related to the elastic coupling, but rather to the competing next-nearest-neighbor spin-spin coupling of the order of  $0.3J$ , has also been discussed recently.<sup>34</sup>

A possible way to understand the relative weight of the  $q=0$  and AF contribution to local dynamic susceptibility, i.e., to copper  $T_1$ , is to perform the oxygen  $^{17}\text{O}$  NMR. By the local symmetry, for  $\text{O}(2)$  sites the AF contribution to oxygen  $^{17}T_1^{-1}$  is filtered out, and comparison of copper and oxygen relaxation rates should bring the answer. However, only the oxygen hyperfine shift data are available yet.<sup>35</sup>

Another interesting point raised by the NMR data is the absence of the field dependence of the  $T_{1z}^{-1}$  in the uniform phase. Numerical results for the zero-temperature spectral function perpendicular to the applied field, corresponding to the exact solution for 10 Heisenberg spins  $1/2$  in the magnetic field,<sup>26</sup> are indeed indicative of the field-independent total spectral weight near the zero energy. However, the spectral functions are significantly modified by the presence of the magnetic field, and we are not aware of any direct calculation regarding the field dependence of  $T_1$ . Note that a negligible field dependence of  $T_1$  has also been found by Cu NMR in another spin- $1/2$  one-dimensional antiferromagnet,  $\text{Sr}_2\text{CuO}_3$ .<sup>36</sup> These results concern rather a low temperature  $k_B T/J \lesssim 0.1$ , and they are thus complementary to our  $k_B T/J > 0.1$  data in the  $U$  phase of  $\text{CuGeO}_3$ . According to the temperature range involved and the values of hyperfine couplings, the  $\text{Sr}_2\text{CuO}_3$  data concern the pure AF-fluctuation contribution to  $T_1^{-1}$ . They are also found in quantitative accord with theoretical predictions.

Finally, the low-temperature  $T_{1z}^{-1}$  NMR data in the dimerized phase clearly reflect the magnetic-field dependence of the energy gap. In an attempt to interpret these data, we discussed several theoretically proposed processes. The three-magnon process<sup>28</sup> predicts an activation energy to be twice the gap value, while the experimental activation energy is rather close to the gap as determined by neutrons. Using the one- (dressed) magnon process<sup>29,30</sup> to fit the data, we found experimentally that the damping  $\Gamma$  of this magnon is at most weakly temperature dependent. However, the reasons for this absence of temperature dependence remains to be clarified. In the two-magnon interbranch process<sup>31</sup> a field-independent activation energy is predicted, in contradiction to the data. The two-magnon intrabranched process could explain the observed field dependence of the activation energy, but in this case the magnetic-field dependence of the relaxation does not correspond to the prediction. Moreover, this process is expected to be extremely angle sensitive, which

remains to be verified. In short, the available experimental data do not allow us to conclude which is the correct description; more information should be obtained primarily by the precise angle dependence measurements of relaxation, and also by extending the field-dependence measurements (at low temperature) to cover the lower and zero magnetic field. Note that the above-mentioned two-magnon processes have been discussed<sup>31</sup> in the context of the Haldane  $S=1$  antiferromagnetic chain, and it would be also interesting to reconsider it theoretically in the particular case of a spin-Peierls system in which the excitation spectrum is different.

#### ACKNOWLEDGMENTS

We are indebted to P. Carretta and A. Sandvik for very useful discussions, to J. Chenavas for the determination of the crystalline axes of the samples, and to P. Veillet for the magnetization measurements. The Grenoble High Magnetic Field Laboratory is ‘‘Laboratoire conventionnée à l’Université Joseph-Fourier de Grenoble.’’ Laboratoire de Spectrométrie Physique is ‘‘Unité Mixte de Recherche No. 5588 du Centre National de la Recherche Scientifique.’’

#### APPENDIX: $T_1$ OF A HEISENBERG CHAIN

Neglecting the logarithmic corrections which are expected to be important for  $T/J < 0.1$  ( $k_B = 1 = \hbar$ ), the dominant contribution to the spin susceptibility of a spin-1/2 Heisenberg AF chain is given by<sup>25</sup>

$$\chi''_{XX} = \chi''_{YY} = \frac{D}{4\pi T} \operatorname{Im} \left[ \rho \left( \frac{\omega - \nu \Delta q}{4\pi T} \right) \rho \left( \frac{\omega + \nu \Delta q}{4\pi T} \right) \right],$$

where  $\rho(x) = \Gamma(1/4 - ix)/\Gamma(3/4 - ix)$ ,  $\nu = \pi J/2$ ,  $\Delta q = q_c - \pi/c$ , and the unknown parameters  $\alpha$  and  $C_\perp$  defined in Ref. 25 are contracted to  $D = \pi \alpha C_\perp^2$ . The zero-temperature limit

$$\chi''_{XX}(T/\omega \rightarrow 0) = D[\omega^2 - (c\Delta q)^2]^{-1/2}$$

can be used to determine the unknown prefactor  $D \sim 1-1.5$ , which is discussed by Müller *et al.*<sup>26</sup> The relaxation rate  $T_1^{-1} = 2(\gamma_n A_\perp)^2 T \sum_q \chi''_{XX}(q, \omega_{\text{NMR}}) / \omega_{\text{NMR}}$  can be calculated using the limit value for  $w \rightarrow 0$  of the integral  $\int_0^\infty \operatorname{Im}[\rho(w-k)\rho(w+k)] dk = w\pi^2$ , which is accurate to less than 1% for  $w < 0.027$ . In this way we recover

$$T_1^{-1} = D \gamma_n^2 A_\perp^2 / (\pi J),$$

which is temperature independent. This is partly due to the approximations used in Ref. 25 in the Fourier transform of the real-space susceptibility  $\chi''_{XX}(r, t)$  to obtain  $\chi''_{XX}(q, \omega)$ . These approximations can be removed if  $T_1$  is calculated directly from the real-space susceptibility using

$$\begin{aligned} \sum_q \chi''_{XX}(q, \omega) / \omega &= \int_0^\infty \sin(\omega t) \chi''_{XX}(r=0, t) / \omega dt \\ &\cong \int_0^\infty t \chi''_{XX}(r=0, t) dt. \end{aligned}$$

The temperature dependence of  $T_1^{-1}$  is then given by the integral

$$\begin{aligned} I(\tau) &= 4\pi^{-2} \int_0^\infty t^3 [(\tau^2 + t^2) \sinh(t)]^{-1} dt \\ &= 1 - 2\tau/\pi + O(\tau^2), \end{aligned}$$

which multiplies the constant  $T_1^{-1}$  value derived from  $\chi''_{XX}(q, \omega)$ :

$$T_1^{-1} = I(2\alpha T/J) D \gamma_n^2 A_\perp^2 / (\pi J).$$

Comparing this analytical expression for the AF contribution to  $T_1^{-1}$ , to the Monte Carlo result of A Sandvik<sup>27</sup> [for the case where  $B$  is chosen to ensure the filtering of the  $q=0$  contribution, i.e., to make  $A_\perp(q=0)=0$ ], we find that parameters  $\alpha=1.3$  and  $D=1.6$  provide a perfect fit to the numerical data in the temperature range  $0.1 \leq T/J \leq 0.4$ .

<sup>1</sup>M. Hase, I. Terasaki, and K. Uchinokura, Phys. Rev. Lett. **70**, 3651 (1993).

<sup>2</sup>see J. W. Bray, L. V. Interrante, I. S. Jacobs, and J. C. Bonner, in *Extended Linear Chain Compounds*, edited by J. C. Miller (Plenum, New York, 1982), p. 353.

<sup>3</sup>A. I. Buzdin and L. N. Bulaevskii, Sov. Phys. Usp. **23**, 409 (1980).

<sup>4</sup>P. Pincus, Solid State Commun. **9**, 1971 (1971); E. Pytte, Phys. Rev. B **10**, 2039 (1974).

<sup>5</sup>D. Bloch, J. Voiron, and L. J. De Jongh, in *Proceedings of the International Symposium on High Field Magnetism*, edited by M. Dake (North-Holland, Amsterdam, 1983), p. 19.

<sup>6</sup>A. Revcolevschi and G. Dhalenne, Adv. Mater. **5**, 9657 (1993).

<sup>7</sup>L. P. Regnault, M. Aïin, B. Hennion, G. Dhalenne, and A. Revcolevschi, Phys. Rev. B **53**, 5579 (1996).

<sup>8</sup>M. Nishi, O. Fujita, and J. Akimitsu, Phys. Rev. B **50**, 6508 (1994).

<sup>9</sup>J. P. Pouget *et al.*, Phys. Rev. Lett. **72**, 4037 (1995); K. Hirota, D. E. Cox, J. E. Lorentzo, G. Shirane, and J. M. Tranquada, *ibid.* **73**, 736 (1995).

<sup>10</sup>V. Kiryukhin and B. Keimer, Phys. Rev. B **52**, R704 (1995); V. Kiryukhin, B. Keimer, J. P. Hill, and A. Vigliante, Phys. Rev. Lett. **76**, 4608 (1996).

<sup>11</sup>Y. Fagot-Revurat, M. Horvatić, C. Berthier, P. Ségransan, G. Dhalenne, and A. Revcolevschi, Phys. Rev. Lett. **77**, 1861 (1996).

<sup>12</sup>M. Itoh, S. Hirashima, and K. Motoya, Phys. Rev. B **52**, 3410 (1995).

<sup>13</sup>M. Itoh, M. Sugahara, T. Yamauchi, and Y. Ueda, Phys. Rev. B **53**, 11 606 (1996).

<sup>14</sup>M. Horvatić, J. Phys. Condens. Matter **4**, 5811 (1992).

<sup>15</sup>K. Le Dang, G. Dhalenne, J. P. Renard, A. Revcolevschi, and P. Veillet, Solid State Commun. **91**, 924 (1994).

<sup>16</sup>J. Kikuchi, H. Yasuoka, M. Hase, Y. Sasago, and K. Uchinokura, J. Phys. Soc. Jpn. **63**, 872 (1994).

<sup>17</sup>J. A. Gillet, T. Auler, M. Horvatić, C. Berthier, Y. Berthier, P. Ségransan, and J. Y. Henry, Physica C **235-240**, 1667 (1994).

<sup>18</sup>Y. Fagot-Revurat *et al.* (unpublished).

<sup>19</sup>M. Horvatić, C. Berthier, Y. Berthier, P. Ségransan, P. Butaud,

- W. G. Clark, J. A. Gillet, and J. Y. Henry, *Phys. Rev. B* **48**, 13 848 (1993).
- <sup>20</sup>Courtesy of P. Veillet; this magnetization measurement was performed on a single crystal of the same origin and quality as our samples.
- <sup>21</sup>S. Oseroff, S. W. Cheong, A. Fondado, B. Aktas, and Z. Fisk, *J. Appl. Phys.* **75**, 6819 (1994).
- <sup>22</sup>Abraham and B. Bleaney, *Electronic Paramagnetic Resonance of Transition Ions* (Clarendon, Oxford, 1970), Chap. 7.16.
- <sup>23</sup>M.-H. Julien, P. Carretta, M. Horvatić, C. Berthier, Y. Berthier, P. Ségransan, A. Carrington, and D. Colson, *Phys. Rev. Lett.* **76**, 4238 (1996).
- <sup>24</sup>E. Ehrenfreund, E. F. Rybaczewski, A. F. Garito, and A. J. Heeger, *Phys. Rev. B* **7**, 421 (1973).
- <sup>25</sup>H. J. Schulz, *Phys. Rev. B* **34**, 6372 (1986).
- <sup>26</sup>G. Müller, H. Thomas, H. Beck, and J. C. Bonner, *Phys. Rev. B* **24**, 1429 (1981).
- <sup>27</sup>A. W. Sandvik, *Phys. Rev. B* **52**, R9831 (1995).
- <sup>28</sup>E. Ehrenfreund and L. S. Smith, *Phys. Rev. B* **16**, 1870 (1977).
- <sup>29</sup>P. Gaveau, J. P. Boucher, L. P. Regnault, and J. P. Renard, *Europhys. Lett.* **12**, 647 (1990).
- <sup>30</sup>N. Fujiwara, T. Goto, S. Maegawa, and T. Kohmoto, *Phys. Rev. B* **47**, 11 860 (1993).
- <sup>31</sup>J. Sagi and I. Affleck, *Phys. Rev. B* **53**, 9188 (1996).
- <sup>32</sup>T. M. Brill, J. P. Boucher, J. Voiron, G. Dhalenne, A. Revcolevschi, and J. P. Renard, *Phys. Rev. Lett.* **73**, 1545 (1994).
- <sup>33</sup>K. Okamoto, *J. Phys. Soc. Jpn.* **56**, 912 (1987).
- <sup>34</sup>G. Castilla, S. Chakravarty, and V. J. Emery, *Phys. Rev. Lett.* **75**, 1823 (1995).
- <sup>35</sup>M. Itoh, M. Sugahara, S. Hirashima, T. Yamauchi, and Y. Ueda, *Physica C* **263**, 486 (1996).
- <sup>36</sup>M. Takigawa, N. Motoyama, H. Eisaki, and S. Uchida, *Phys. Rev. Lett.* **76**, 4612 (1996).